Oncogene (2016) **35,** 3399–3409
© 2016 Macmillan Publishers Limited All rights reserved 0950-9232/16
www.nature.com/onc

ORIGINAL ARTICLE

Inhibition of caspases primes colon cancer cells for 5-fluorouracil-induced TNF-α-dependent necroptosis driven by RIP1 kinase and NF-κB

M Oliver Metzig[1,2], D Fuchs[1,2], KE Tagscherer[2], H-J Gröne[3], P Schirmacher[1] and W Roth[1,2,4]

Resistance towards the drug 5-fluorouracil (5-FU) is a key challenge in the adjuvant chemotherapy of colorectal cancer (CRC), and novel targeted approaches are required to improve the therapeutic outcome. Necroptosis is a recently discovered form of programmed cell death, which depends on receptor interacting protein 1 (RIP1) and particularly occurs under caspase-deficient conditions. The targeted induction of necroptosis represents a promising strategy to overcome apoptosis resistance in cancer. The aim of this study was to systematically explore the usage of pan-caspase inhibitors to sensitize resistant CRC cells for 5-FU. We found that pan-caspase inhibitors facilitated 5-FU-induced necroptosis, which was mediated by autocrine secretion of tumor necrosis factor α (TNF-α). TNF-α production was driven by nuclear factor κB (NF-κB) and required RIP1 kinase. *In vivo* xenograft experiments showed that the novel pan-caspase inhibitor IDN-7314 in combination with 5-FU synergistically blocked tumor growth. *Ex vivo* experiments with fresh human CRC tissue specimens further indicated that a subgroup of patients could benefit from combinatory treatment. Thereby, elevated levels of secreted TNF-α and expression of components of the necroptotic pathway might help to predict the sensitivity to pro-necroptotic therapies. Together, our results shed new light on the molecular regulation of necroptosis by NF-κB and RIP1. Moreover, we identify necroptotic cell death as an important effector mechanism of 5-FU-mediated anti-tumoral activity. On the basis of this study, we propose pan-caspase inhibitors as a novel approach in the adjuvant chemotherapy of CRC.

Oncogene (2016) **35,** 3399–3409; doi:10.1038/onc.2015.398; published online 2 November 2015

INTRODUCTION

Colorectal cancer (CRC) is the third most common cancer and the fourth leading cause of death from cancer worldwide.[1] The therapeutic mainstay is surgery combined with radiotherapy or chemotherapy depending on tumor site and progression of disease.[2–4] 5-Fluorouracil (5-FU) is the standard chemotherapeutic agent for advanced CRC[4] and—in combination with newer substances—initial response rates of 40–50% are achieved.[5] Different factors are believed to contribute towards 5-FU resistance, such as aberrant expression of thymidine synthetase[6] and p53 mutations.[7,8] Restoring 5-FU sensitivity in resistant tumors remains an important challenge in the chemotherapy of CRC.

Although 5-FU has traditionally been studied for its potential to induce apoptosis, several alternative forms of programmed cell death have gained attention in the meantime.[9] One prominent example is necroptosis, which is a regulated form of necrosis. Similarly to apoptosis, necroptosis is mediated by cascade-like signaling pathways, but does not require the activation of caspases.[10] The best-characterized form of necroptosis depends on receptor interacting protein 1 (RIP1) kinase, a key player within the tumor necrosis factor α receptor 1 (TNFR1) signaling network to determine cell death and survival.[11,12] Necrostatins, RIP1-specific kinase inhibitors, potently block RIP1-dependent necroptosis.[13] Most types of cancer cells are resistant towards TNFR1-mediated apoptosis, for example, owing to previous activation of NF-κB.[14,15] Thereby, the targeted induction of necroptosis has been proposed as a strategy to overcome apoptosis resistance.[16] For example, second mitochondrial activator of caspases (Smac) mimetics can potently induce TNF-α-dependent necroptosis in cancer cell types, especially in the presence of pan-caspase inhibitors such as Z-VAD.[17–19] In addition, the potential of chemotherapeutics to induce necroptosis is of critical clinical interest and needs to be explored.

In this study, we show that pan-caspase inhibitors can sensitize resistant CRC cells to 5-FU-induced necroptosis. Functional *in vitro* experiments revealed that the induction of necroptosis required a positive TNF-α feedback loop, which was driven by RIP1 kinase and NF-κB. On the basis of *in vivo* and *ex vivo* approaches, we propose the combination of 5-FU with pan-caspase inhibitors as a novel therapeutic principle to overcome chemoresistance in CRC.

RESULTS

5-FU induces necroptosis in CRC cells in the presence of caspase inhibitors

In initial experiments, we investigated the differential effects of 5-FU in a panel of human CRC cell lines. In HCT116, low doses of 5-FU potently reduced the amount of vital adherent cells (Figure 1a, first panel). The extent of cell death was substantially decreased by the pan-caspase inhibitor Z-VAD—indicating that

[1]Institute of Pathology, University of Heidelberg, Heidelberg, Germany; [2]Molecular Tumor Pathology, German Cancer Research Center, Heidelberg, Germany; [3]Cellular and Molecular Pathology, German Cancer Research Center, Heidelberg, Germany and [4]Institute of Pathology, University Medical Center Mainz, Mainz, Germany. Correspondence: Professor W Roth, Institute of Pathology, University Medical Center Mainz, Langenbeckstr. 1, 55131 Mainz, Germany.
E-mail: Wilfried.Roth@unimedizin-mainz.de
Received 20 April 2015; revised 3 August 2015; accepted 22 August 2015; published online 2 November 2015

5-FU-induced cell death was at least partially due to apoptosis. In contrast, HT29 cells required much higher doses of 5-FU to attain a similar cytotoxic effect (Figure 1a, second panel). As addition of Z-VAD led to further sensitization towards 5-FU, we suggested that HT29 underwent caspase-independent necroptosis. In SW480 cells, 5-FU in the presence or absence of Z-VAD had only minor

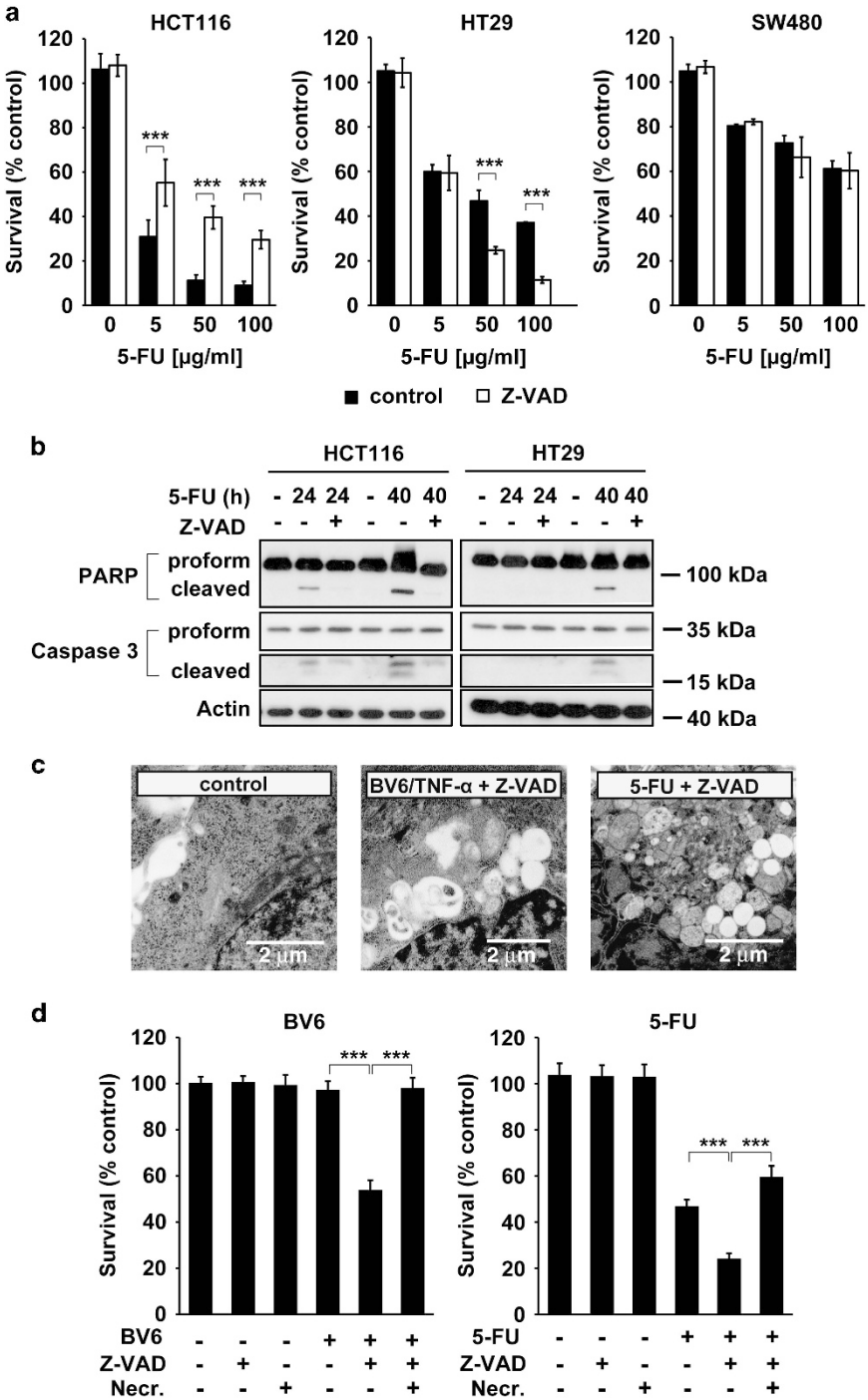

Figure 1. The pan-caspase inhibitor Z-VAD sensitizes colon carcinoma cells towards 5-FU. (**a**) Effects of 5-FU and Z-VAD on human CRC cell lines. Pre-treatment with Z-VAD (50 µM) for 2 h was followed by addition of 5-FU (50 µg/ml) for 48 h. Percentage of cells treated with DMSO. Mean obtained from three independent biological replicates with three technical replicates each (±s.d., two-sided Student's *t*-test, ***$P < 0.001$). (**b**) 5-FU induces the cleavage of PARP and caspase 3 in HCT116, but not in HT29 cells. After treatment as described in (**a**) for the indicated durations, cell lysates were analyzed via western blot. Actin: loading control. (**c**) Ultrastructural analysis of necroptosis in HT29 via electron microscopy. Pre-treatment with Z-VAD (50 µM) for 2 h was followed by the addition of BV6 (0.6 µM) and TNF-α (25 ng/ml) for 12 h, or 5-FU (50 µg/ml) for 40 h. Compared with control cells (DMSO), both treatments resulted in prominent enlargement of mitochondria and vacuolization of cellular organelles in a representative subpopulation of cells. Scale bar: 2 µm. For additional pictures, see Supplementary Figure 2. (**d**) Necrostatin-1 blocks BV6- and 5-FU-induced necroptosis. HT29 were pre-treated with Z-VAD (50 µM) and/or Necrostatin-1 (20 µM) for 2 h, followed by stimulation with BV6 (0.6 µM) or 5-FU (50 µg/ml) for 48 h (mean of three independent experiments with three technical replicates each ±s.d., two-sided Student's *t*-test, ***$P < 0.001$).

© 2016 Macmillan Publishers Limited

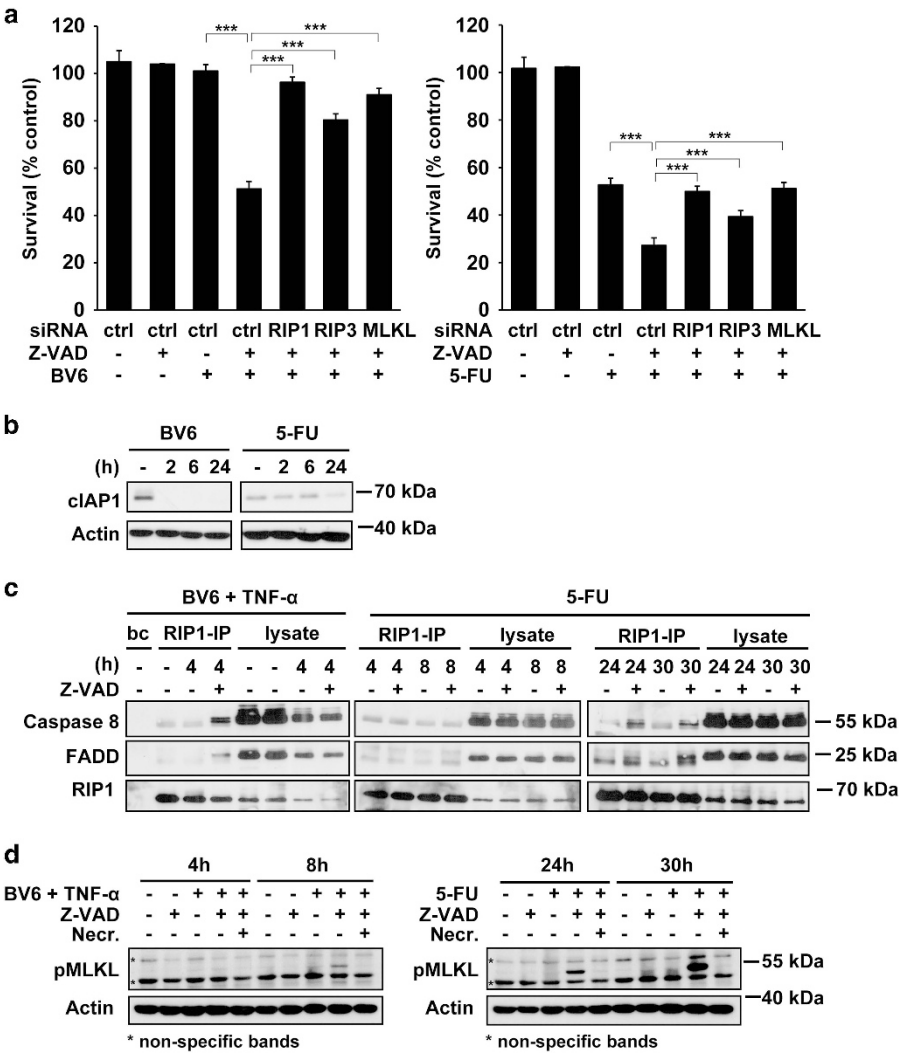

Figure 2. 5-FU and Z-VAD-induced necroptosis depends on RIP1 and RIP3. (**a**) Effects of RIP1, RIP3 or MLKL knockdown on necroptosis. HT29 cells were transfected with siRNAs, pre-treated with Z-VAD (50 μM) for 2 h, and BV6 (0.6 μM) or 5-FU (50 μg/ml) was added for 48 h. Mean percentage of control (ctrl, scrambled siRNA and DMSO), obtained from three independent biological replicates with three technical replicates each (±s.d., two-sided Student's *t*-test, ***$P < 0.001$). (**b**) Decreased cIAP1 protein levels after treatment with BV6 or 5-FU. HT29 cells were treated with BV6 (0.6 μM) or 5-FU (50 μg/ml) for indicated times and cIAP1 levels were measured via western blot. Actin: loading control. (**c**) Co-immunoprecipitation of RIP1 after induction of necroptosis. HT29 cells were pre-treated with Z-VAD (50 μM) for 2 h, and stimulated with BV6 (0.6 μM) and TNF-α (25 ng/ml), or 5-FU (50 μg/ml) for indicated durations. After pull-down of RIP1, precipitates were analyzed via western blot. Bc: bead control. (**d**) pMLKL levels after the induction of necroptosis. HT29 cells were treated as described in (**c**) and levels of phosphorylated MLKL were analyzed via western blot. Asterisk marks non-specific bands detected by the antibody. Actin: loading control.

effects (Figure 1a, third and fourth panel). Whereas apoptosis of HCT116 cells was accompanied by cleavage of PARP and caspase 3 (Figure 1b, left panel), the synergistic effects of 5-FU and Z-VAD in HT29 cells were independent from PARP and caspase 3 cleavage (Figure 2b, right panel). Flow cytometry confirmed that 5-FU induced characteristic signs of apoptosis in HCT116, which was blocked by Z-VAD (Supplementary Figure 1A). In contrast, co-treatment of 5-FU and Z-VAD led to primary signs of necrosis in HT29 cells (Supplementary Figure 1B).

Smac mimetics have previously been shown to trigger TNF-α-dependent necroptosis in HT29 cells under caspase-deficient conditions.[18] Thus, we analyzed 5-FU and Z-VAD-induced cell death in analogy to treatment with the Smac mimetic BV6, TNF-α and Z-VAD. Ultrastructural analysis revealed that both treatments resulted in a similar necrosis-like phenotype with characteristic morphological changes (Figure 1c, Supplementary Figure 2). In line with previous findings, BV6 and Z-VAD-induced necroptosis was significantly rescued by the RIP1-specific kinase inhibitor Necrostatin-1 (Figure 1d, left panel), which was even more prominent in the presence of TNF-α (Supplementary Figure 3A).[18] Importantly, Necrostatin-1 also rescued cells from 5-FU- and Z-VAD-induced death (Figure 1d, right panel). Together, these results indicated that Z-VAD sensitized HT29 cells for 5-FU-induced necroptosis.

5-FU and Z-VAD-induced necroptosis depends on RIP1, RIP3 and TNFR1

In HT29 cells, Smac mimetics/TNF-α-induced necroptosis is mediated via RIP1, RIP3 and the downstream target MLKL.[18,20] Indeed, knockdown of RIP1, RIP3 or MLKL significantly rescued cells from BV6 (Figure 2a, left panel) or 5-FU plus Z-VAD-induced necroptosis (Figure 2a, right panel; for short interference RNA (siRNA) effects see Supplementary Figures 3B and D). Comparable effects were obtained with the MLKL inhibitor Necrosulfonamide,[20] or the RIP3-specific kinase inhibitor GSK'872[21] (Supplementary

© 2016 Macmillan Publishers Limited

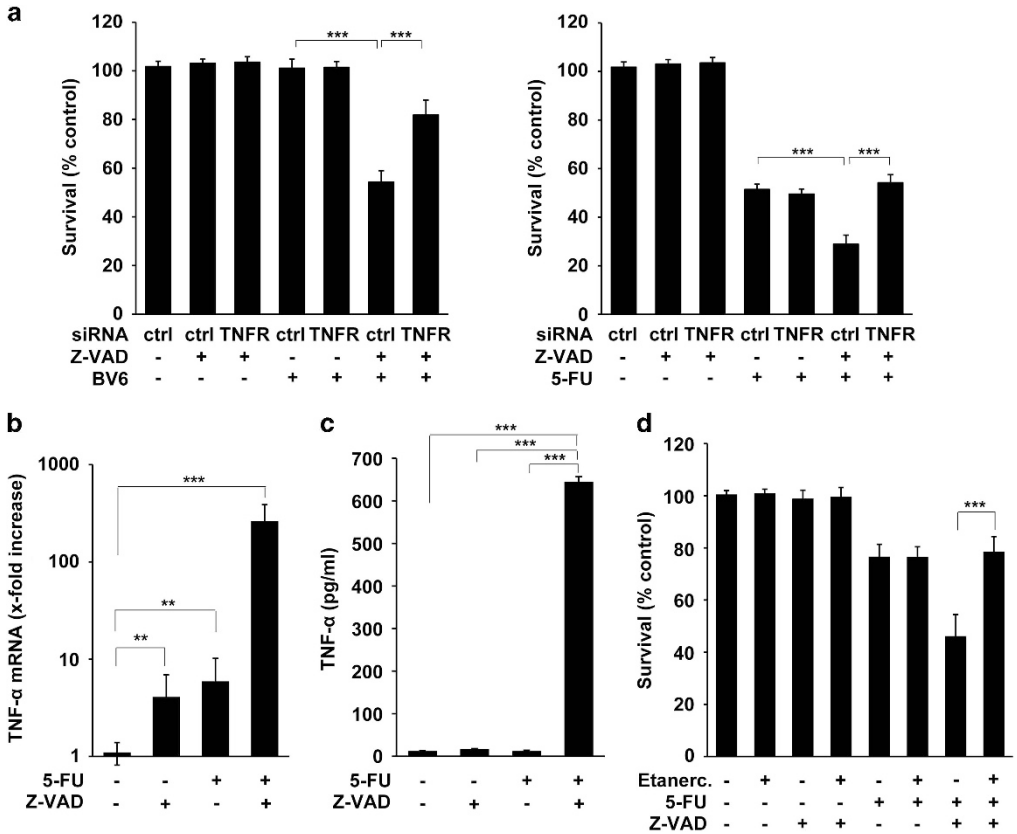

Figure 3. 5-FU- and Z-VAD-induced necroptosis depends on TNFR1 and autocrine TNF-α production. (**a**) Effects of TNFR1 knockdown on necroptosis. HT29 cells were transfected with siRNA against TNFR1, pre-treated with Z-VAD (50 μM) for 2 h, and BV6 (0.6 μM) and TNF-α (25 ng/ml), or 5-FU (50 μg/ml) was added for 48 h. Mean percentage of control, obtained from three independent experiments with three technical replicates each (±s.d., two-sided Student's *t*-test, $^{***}P < 0.001$). (**b**) 5-FU and Z-VAD induced increased mRNA levels of TNF-α as relatively quantified via qRT–PCR. HT29 cells were treated with Z-VAD (50 μM) for 2 h, and 5-FU (50 μg/ml) for 24 h. Mean fold increase compared with control (scrambled siRNA and DMSO), obtained from three independent biological replicates with two technical replicates each (±s.d., two-sided Student's *t*-test, $^{**}P < 0.01$, $^{***}P < 0.001$). (**c**) TNF-α production induced by 5-FU and Z-VAD as quantified in cell culture supernatants by ELISA. HT29 cells were treated as described in (**a**). Means of one out of three representative independent experiments with two technical replicates each (±s.d., two-sided Student's *t*-test, $^{***}P < 0.001$). (**d**) Effect of TNF-α antagonist Etanercept on necroptosis. HT29 cells were treated with Z-VAD and 5-FU as described in (**a**), in the presence or absence of Etanercept (50 μg/ml), and remaining cells were quantified via crystal violet assay. Mean percentage of control cells (DMSO), obtained from three independent experiments with three technical replicates each (±s.d., two-sided Student's *t*-test, $^{***}P < 0.001$).

Figure 3E). However, in our hands, knockdown of RIP3 and GSK'872 had a slightly reduced effect compared with the other siRNAs and inhibitors.

Smac mimetics/TNF-α-induced cell death is triggered by the degradation of cIAPs, which favors the transition of complex I (RIP1/TRADD/TRAF2) into complex II (RIP1/TRADD/caspase 8/FADD) upon internalization of TNFR1.[14,15,18] Similar to BV6, 5-FU treatment reduced cIAP1 protein levels (Figure 2b), which might occur in response to genotoxic stress (Supplementary Figure 3 F).[22,23] Furthermore, the addition of Z-VAD resulted in stabilization of a protein complex containing RIP1, caspase 8 and FADD (Figure 2c, Supplementary Figure 3G). Moreover, stabilized binding between RIP1 and RIP3 was detected (Supplementary Figure 3H), accompanied by the phosphorylation of MLKL (Figure 2d). Further experiments revealed that knockdown of TNFR1 rescued HT29 cells from BV6/TNF-α (Figure 3a, left panel) or 5-FU (Figure 3a, right panel) plus Z-VAD-induced necroptosis (for siRNA effects, see Supplementary Figures 3I and J).

Thus, we assumed that 5-FU-mediated loss of cIAP1 favored TNFR1-dependent formation of complex II, which was likely stabilized by Z-VAD and induced downstream necroptosis upon recruitment of RIP3 and phosphorylation of MLKL.

5-FU and Z-VAD trigger necroptosis via autocrine TNF-α production driven by NF-κB

As knockdown of TNFR1 potently blocked 5-FU and Z-VAD-induced necroptosis, we hypothesized that endogenous TNF-α could have a major role in this mechanism. Indeed, 5-FU and Z-VAD treatment led to a marked increase of TNF-α production (Figures 3b and c), whereas 5-FU or Z-VAD alone had only a minor effect (Figure 3b). Furthermore, co-treatment with Etanercept, a neutralizing TNF-α antibody, rescued HT29 cells from necroptosis (Figure 3d). Interestingly, 5-FU treatment was accompanied by increased expression of TNFR1 on the cell surface, which might sensitize cells towards TNF-α (Supplementary Figure 3K). We concluded that autocrine TNF-α production and a positive TNFR1 feedback loop were required to trigger necroptosis.

NF-κB is an important source of TNF-α and can be activated by various stimuli including chemotherapeutics and genotoxic stress.[15,24] We investigated NF-κB activity during 5-FU and Z-VAD-induced necroptosis. Indeed, phosphorylation of IκBα (Figure 4a) and nuclear translocation of RelA and p52 (Supplementary Figure 4A) were detected 24 h after 5-FU and Z-VAD treatment. Whereas single treatment with 5-FU or Z-VAD had only a slight upregulative effect, combination treatment with

© 2016 Macmillan Publishers Limited

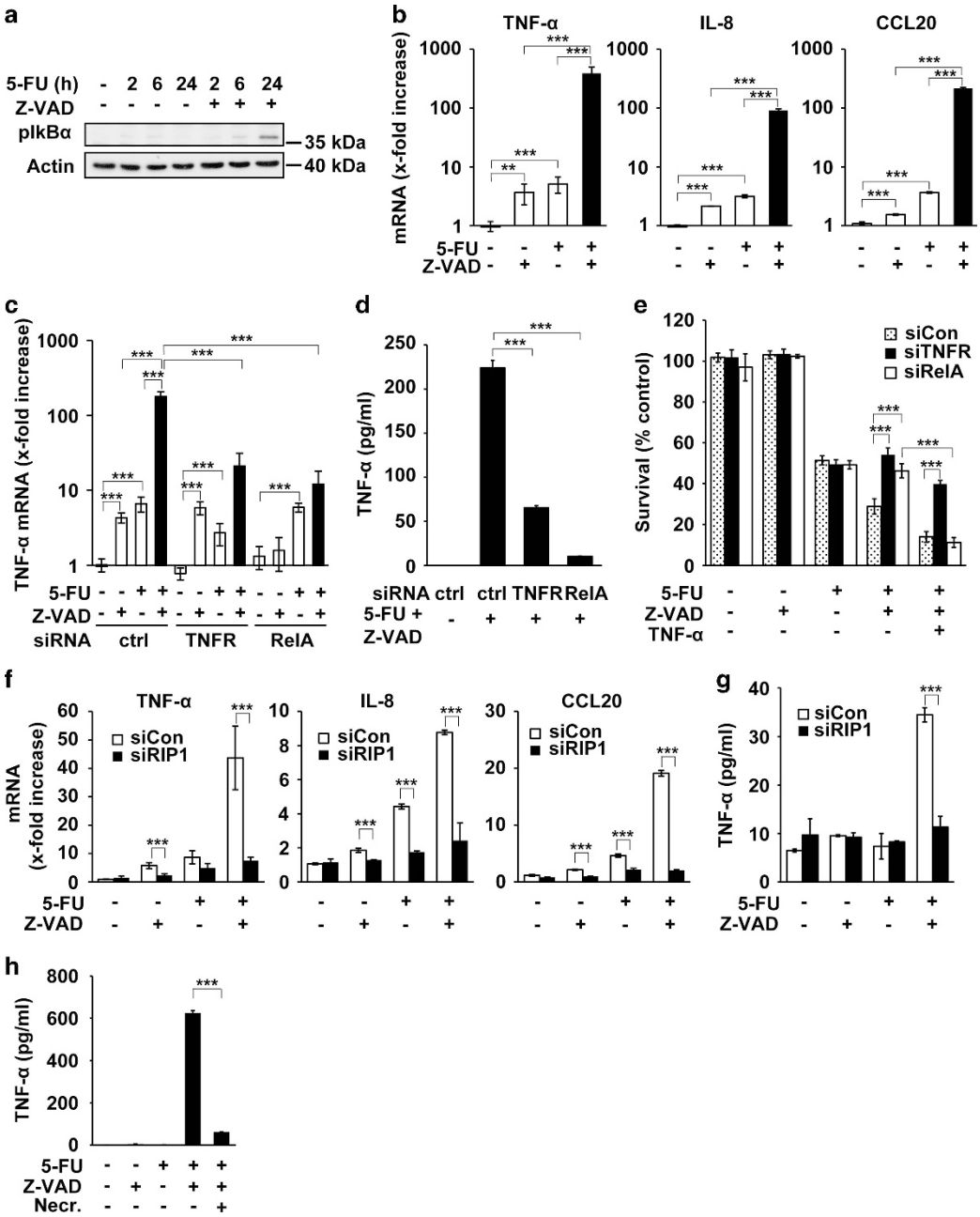

Figure 4. Autocrine TNF-α production is driven by NF-κB and RIP1 kinase. (**a**) pIκBα levels after treating HT29 cells with Z-VAD (50 μM) and 5-FU (50 μg/ml) for indicated durations as analyzed by western blot. Actin: loading control. (**b**) Elevated mRNA levels of NF-κB target genes after the induction of necroptosis. HT29 cells were treated for 24 h as described in (**a**), and mRNA levels of TNF-α, IL-8 and CCL20 were quantified via qRT–PCR. Mean fold increase compared with control (ctrl, DMSO), obtained from three independent biological replicates with two technical replicates each (±s.d., two-sided Student's *t*-test, $^{**}P < 0.01$, $^{***}P < 0.001$). (**c**) Effects of TNFR1 or RelA knockdown on TNF-α mRNA expression as quantified by qRT–PCR. HT29 cells were transfected with indicated siRNAs and treated as specified in (**a**) for 24 h. Mean fold increase compared with control (ctrl, scrambled siRNA and DMSO), obtained from three independent experiments with two technical replicates each (±s.d., two-sided Student's *t*-test, $^{***}P < 0.001$). (**d**) TNF-α secretion after knockdown of TNFR1 or RelA. Cell culture supernatants from (**c**) were analyzed by ELISA. Means of one out of three representative independent experiments with two technical replicates each (±s.d., two-sided Student's *t*-test, $^{***}P < 0.001$). (**e**) Effects of TNFR or RelA knockdown on necroptosis. HT29 cells were transfected with indicated siRNAs and treated with Z-VAD (50 μM) and 5-FU (50 μg/ml) for 48 h in the presence or absence of TNF-α (25 μg/ml). Mean percentage of control (siCon, scrambled siRNA and DMSO) obtained from three independent experiments with three technical replicates each (±s.d., two-sided Student's *t*-test, $^{***}P < 0.001$). (**f**) Depletion of NF-κB target gene transcription after knockdown of RIP1. HT29 cells were transfected with the indicated siRNAs and treated for 24 h as described in (**a**). mRNA levels of TNF-α, IL-8 and CCL20 were quantified via qRT–PCR. Mean fold increase compared with control (siCon, scrambled siRNA and DMSO), obtained from three independent biological replicates with two technical replicates each (±s.d., two-sided Student's *t*-test, $^{***}P < 0.001$). (**g**) TNF-α secretion after knockdown of RIP1. Cell culture supernatants from (**f**) were analyzed by ELISA. Means of three representative independent experiments with two technical replicates each (±s.d., two-sided Student's *t*-test, $^{***}P < 0.001$). (**h**) Effect of Necrostatin-1 on TNF-α secretion. HT29 cells were pre-treated with Z-VAD (50 μM) and/or Necrostatin-1 (20 μM) for 2 h, followed by stimulation with 5-FU (50 μg/ml) for 24 h. Cell culture supernatants were analyzed by ELISA. Data show means of three representative experiments with two technical replicates each (±s.d., two-sided Student's *t*-test, $^{***}P < 0.001$).

© 2016 Macmillan Publishers Limited

5-FU and Z-VAD resulted in robust transcription of NF-κB target genes, such as TNF-α, IL-8 and CCL20 (Figure 4b), while other target genes, such as IκBα, $cFLIP_{long}$, XIAP and cIAP1, were less affected (Supplementary Figure 4b). Furthermore, downregulation of TNFR1 or RelA via siRNA blocked robust autocrine TNF-α production (Figures 4c and d; for siRNA effects, see Supplementary Figures 3I and J). Accordingly, the rescuing effect of siRelA (Figure 4e) or MLN-4924 (Supplementary Figure 4C), a small molecule inhibiting the degradation of IκBα, was abolished by recombinant TNF-α. Interestingly, HCT116 and SW480 cells lacked elevated levels of TNF-α or NF-κB in response to 5-FU and Z-VAD (Supplementary Figures 4D and F). However, SW480 cells could not be sensitized towards 5-FU and Z-VAD-induced necroptosis via the addition of recombinant TNF-α (data not shown) suggesting that other factors might be involved to determine their necroptosis-sensitivity. In fact, HCT116 and SW480 cells lacked the expression of RIP3 (Supplementary Figure 4G), which is probably significant in this context as previously shown.[18]

Importantly, the combination of 5-FU with the alternative pan-caspase inhibitor IDN-7314 led to robust activation of NF-κB target gene transcription, autocrine TNF-α production and necroptosis (Supplementary Figures 5A and C), indicating that these effects were not specific for Z-VAD. However, Z-DEVD (inhibitor of caspase 3/7), Z-VEID (inhibitor of caspase 6) and Z-IETD (inhibitor of caspase 8) did not exert the same effects (Supplementary Figure 5D).

From these experiments, we concluded that 5-FU and pan-caspase inhibitors employ robust NF-κB-dependent production of TNF-α to induce necroptosis in HT29 cells.

Activation of NF-κB and autocrine TNF-α production by 5-FU and Z-VAD depend on RIP1 kinase

It has previously been shown that Z-VAD triggers autocrine TNF-α production via EDD, RIP1 kinase and JNK in certain cells.[25] We found that knockdown of RIP1 impaired transcription of NF-κB target genes and autocrine TNF-α production in response to 5-FU and/or Z-VAD in HT29 cells (Figures 4f and g). Furthermore, Necrostatin-1 led to a significant decrease of TNF-α production and NF-κB target gene transcription (Figure 4h, Supplementary Figure 6A). However, knockdown of constitutively binding EDD was not sufficient to block robust activation of NF-κB or TNF-α production resulting from 5-FU and Z-VAD treatment (Supplementary Figures 6B and D). In line with this, necroptotic death of HT29 cells was not impaired by the knockdown of EDD or JNK (Supplementary Figures 6E and F). We concluded that in this case, RIP1 kinase employs an alternative mechanism to induce autocrine TNF-α production. As knockdown of RIP3 led to increased TNF-α production (Supplementary Figures 6C and D), we suggested that RIP1 kinase-dependent stimulation of NF-κB occurs upstream of RIP3-induced necroptosis. Interestingly, knockdown of caspase 8 potently diminished the activation of NF-κB and TNF-α production (Supplementary Figures 6G and H). From this, we propose that in HT29 cells, RIP1 kinase possibly cooperates with caspase 8 to trigger 5-FU and Z-VAD-induced NF-κB signaling and TNF-α production.

In vivo and *ex vivo* evidence for the usage of pan-caspase inhibitors as novel anti-tumor agents in CRC

Next, we sought to investigate the *in vivo* anti-cancer potential of 5-FU combined with IDN-7314. To this end, mice bearing HT29 xenograft tumors were treated with 5-FU and/or IDN-7314. Macroscopic and microscopic examination revealed that combinatory treatment of 5-FU and IDN-7314 for 3 weeks synergistically resulted in decreased tumor size (Figures 5a and b) and increased signs of tumor regression (Figure 5c). Significant changes of proliferative activity in vital tumor areas were not detected (Supplementary Figure 6I).

To further evaluate caspase inhibitors as potential anti-cancer agents, we used an *ex vivo* tissue-slice culture model for CRC. As significantly elevated levels of lactate dehydrogenase (LDH) were released by HT29 cells undergoing necroptosis (Figure 6a), LDH was used as a marker of tumor tissue breakdown, and as a surrogate marker for anti-tumoral efficacy.[26] Fresh tissue specimens from CRC patients ($n = 13$) were incubated with 5-FU or 5-FU plus Z-VAD for 48 h. The tested tumors showed different responses to treatment (Figure 6b). Four of 13 colon carcinoma samples exhibited a $\geqslant 1.5$-fold LDH increase after 5-FU single therapy (Figure 6b), accompanied by significantly elevated levels of cleaved caspase 3 (Supplementary Figure 7A), which we interpreted as indicative for apoptosis. In contrast, five tumors showed elevated levels of LDH after combinatory treatment (Figure 6b) lacking elevated levels of cleaved caspase 3 (Supplementary Figure 7A), which was suggestive for necroptosis. As *in vitro* experiments revealed that NF-κB-dependent TNF-α levels might be an indicator of necroptosis sensitivity, we compared the levels of released TNF-α and NF-κB activity after treatment with 5-FU and Z-VAD. In fact, significantly elevated levels of released TNF-α were exclusively seen in necroptosis-sensitive carcinoma (Figure 6b). Consistently, increased activation of NF-κB was preferably observed in necroptosis-sensitive cases (Supplementary Figure 7B). In addition, co-expression of components of the necroptotic pathway (caspase 8, RIP1, RIP3 and MLKL) was preferably seen in the subgroup of necroptosis-sensitive cases (Supplementary Figure 7C). Thus, monitoring the activity of TNF-α/NF-κB signaling together with expression levels of components of the necroptotic pathway might potentially be useful to predict the sensitivity towards pro-necroptotic therapy.

Taken together, these data suggest that pan-caspase inhibitors in combination with 5-FU might be a promising novel anti-cancer strategy in resistant CRC.

DISCUSSION

5-FU resistance is a severe problem in the treatment of CRC.[27] The discovery of necroptosis as an inducible, alternative form of programmed cell death has opened up novel and exciting perspectives to kill resistant cancer cells.[11,28] Several strategies exist to trigger necroptosis: the natural compound shikonin has been shown to bypass deficiencies in apoptosis pathways;[29] inhibition of GSK3B can sensitize resistant p53-mutant colon cancer cells for necroptosis;[30] Smac mimetics and the alkaloid Staurosporine induce necroptosis in acute myeloid leukemia and different carcinoma cell lines.[18,31,32] Interestingly, in some cancer cells, the inhibition of caspases is required to enable necroptosis.[11] Our initial finding was that the pan-caspase inhibitor Z-VAD sensitized resistant HT29 cells to 5-FU-induced cell death. Similarly to the well-established form of necroptosis induced by Smac mimetics and Z-VAD, 5-FU and Z-VAD-mediated necroptosis depended on RIP1 and autocrine TNF-α production. Although Z-VAD alone has been shown to trigger robust TNF-α production in certain cells,[25] in our model, co-stimulation of both 5-FU and Z-VAD was required to sufficiently amplify NF-κB-dependent TNF-α production. In this mechanism, RIP1 kinase seems to have a key role. Interestingly, similar effects were obtained when 5-FU was combined with the alternative pan-caspase inhibitor IDN-7314 indicating that the effects were not specific for Z-VAD. Pan-caspase inhibitors can sufficiently block caspase 8-mediated cleavage of RIP1,[33] and stabilize RIP1-containing protein complexes.[23] From our data, we assume that 5-FU provides an initial, NF-κB-activating stimulus in HT29 cells, for example, by genotoxic stress-related loss of cIAP1,[22,23] and stabilization of NIK.[15,34] At the same time, under caspase-competent conditions, 5-FU induces apoptotic death in a smaller fraction of HT29 cells, which is probably accompanied by localized, caspase 8-dependent degradation of RIP1 and prevents both robust

© 2016 Macmillan Publishers Limited

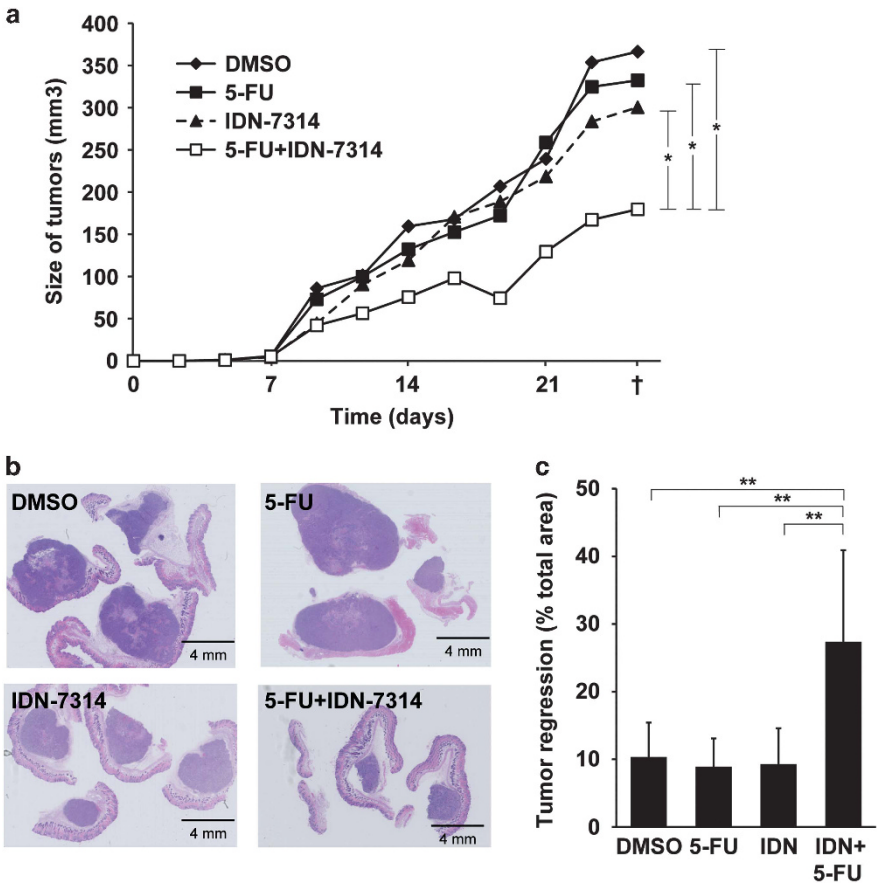

Figure 5. *In vivo* combinatory treatment with the novel pan-caspase inhibitor IDN-7314 and 5-FU. (**a**) Tumor volumes of HT29 xenografts in mice. CD1 nude mice subcutaneously inoculated with HT29 cells (time point 0) received intraperitoneal injections with 5-FU and/or IDN-7314 for 3 weeks, and tumor volumes were measured at regular intervals (DMSO: vehicle control). Mean ($n = 8 \pm$ s.d., two-sided Welch's *t*-test, $^*P < 0.05$). †: mice killed. (**b**) Total histological sections (hematoxylin and eosin) of representative xenograft tumors. ×2 magnification, scale bar: 4 mm. (**c**) Histological tumor sections examined for signs of regression such as sclerosis and necrosis as quantified by Aperio Image Scope software. Regressive areas shown as mean percentage of each tumor's size ($n = 8 \pm$ s.d., two-sided Student's *t*-test, $^{**}P < 0.01$).

activation of NF-κB and necroptosis.[23,33,35] However, in the presence of pan-caspase inhibitors, RIP1-containing protein complexes are stabilized, which can lead to augmented NF-κB signaling.[35] Further engagement of TNFR1 via autocrine TNF-α production can amplify this signal via canonical activation of NF-κB. Ultimately, the stabilization of complex II can mediate necroptosis upon the recruitment of RIP3 in competent HT29 cells.

Our data suggest that RIP1 kinase activity is required for mediation of NF-κB signaling. Thereby, RIP1 kinase might cooperate with a binding partner similarly to EDD.[25] Interestingly, we found that caspase 8 might have a mechanistic function for robust activation of NF-κB, which does not require its enzymatic activity. Indeed, previous studies have shown that pro-domains of caspase 8 can induce NF-κB,[36] for example, through interaction with RIP1, IKK or NIK,[37,38] or as a scaffolding protein.[39] It is possible that RIP1 kinase would be involved in such a process, and also pan-caspase inhibitors might have a contributory function. However, it has also been reported that the loss of caspase 8 can cause severe inflammation, which has been related to increased RIP1 kinase activity and subsequent TNF-α production.[12] Thus, the exact mechanisms and physiological significance of caspase 8 in this context need to be confirmed.

Interestingly, Z-DEVD, Z-VEID and Z-IETD did not lead to robust activation of NF-κB when combined with 5-FU. It has been shown that these substances do not block RIP1 cleavage to the full extent,[33,40] which might provide a possible explanation. However, it has also been reported that RIP1 cleavage can occur in the presence of Z-VAD owing to the localized activation of caspase 8.[23] Moreover, it has recently been shown that limited cleavage can create a truncated version of RIP1, which augmented TRAIL-induced activation of NF-κB in certain cells.[41] Although we observed stabilized binding between RIP1 and caspase 8, fragments of RIP1 were not detected in the presence of Z-VAD (Supplementary Figure 3G). However, whether stabilization of RIP1 is really the crucial event for facilitating TNF-α-dependent necroptosis in HT29 cells and whether caspase 8 is the exclusive target of pan-caspase inhibitors need to be verified by future investigations.

In HCT116 or SW480 cells, neither augmentation of NF-κB nor TNF-α production after 5-FU plus Z-VAD treatment were observed. It is possible that different expression levels of factors that influence the activation status of RIP1 or caspase 8, such as XIAP, FLIP, TRAF or CYLD, might determine their ability to produce autocrine TNF-α, which has previously been shown to have an impact on whether cancer cells can undergo necroptosis or not.[18,42] In addition, HCT116 and SW480 cells lacked expression of RIP3, which probably influences their sensitivity towards necroptosis.[18] Although RIP3 did not seem to be required for TNF-α production, its role for downstream, TNF-α-induced necroptosis in HT29 cells is well-established.[18] Thus, we assume that the slightly reduced rescuing effect of RIP3 knockdown and GSK'872 in our hands was due to technical artifacts. The fact, that knockdown of RIP3 even led to increased NF-κB-dependent TNF-α

© 2016 Macmillan Publishers Limited

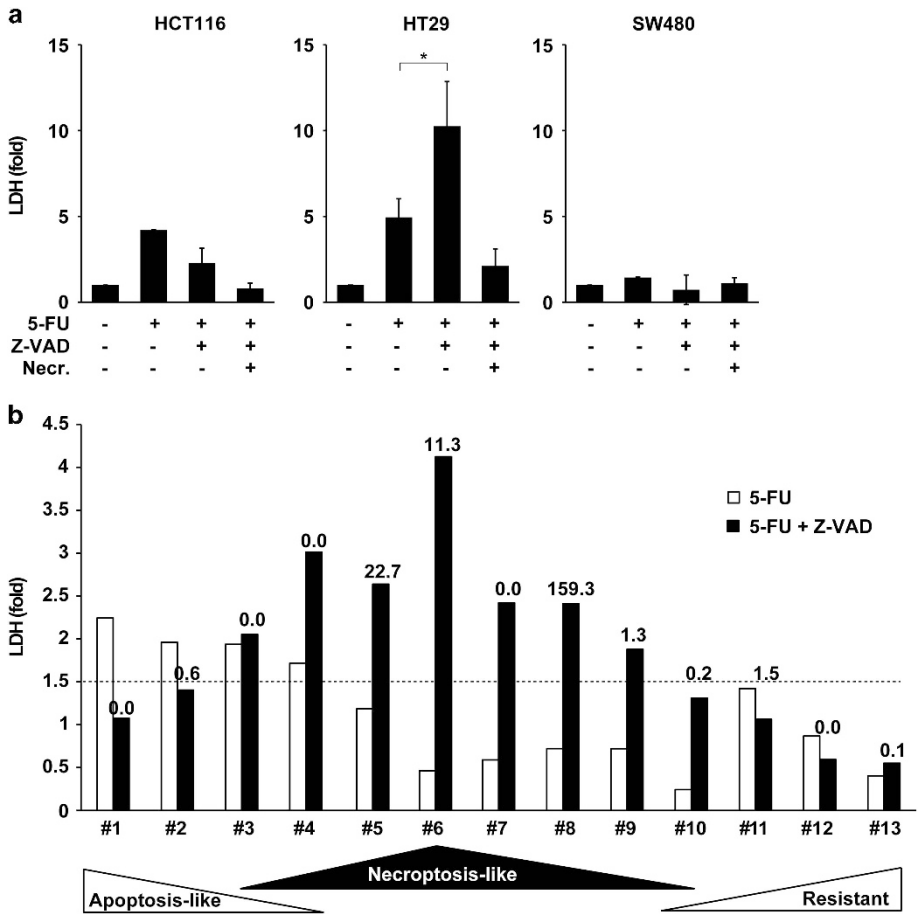

Figure 6. Combinatory treatment with Z-VAD and 5-FU in an *ex vivo* model of CRC. (**a**) Validation of LDH as a marker of tumor cell breakdown. CRC cells were pre-treated with Z-VAD (50 μM) and Necrostatin (20 μM) for 2 h, followed by addition of 5-FU (50 μg/ml) for 48 h. LDH was quantified in cell culture supernatants. Fold increase compared with control (DMSO), obtained from three independent experiments (± s.d., two-sided Student's *t*-test, $*P < 0.05$). (**b**): *Ex vivo* model for human CRC. Fresh sliced tumor specimens of CRC patients ($n = 13$) were pre-treated with Z-VAD (50 μM) for 2 h, and incubated with 5-FU (500 μg/ml) for 48 h. LDH was quantified in tissue culture supernatants and normalized according to tumor content in biopsy. Dashed line marks ⩾1.5-fold LDH increase compared with control (DMSO). Numbers above bars represent x-fold TNF-α increase in the culture supernatants compared with control.

production could indicate that upstream RIP1 is available to form other, NF-κB-inducing protein complexes.

The concept to use caspase inhibitors as anti-cancer agents is novel, and so far, there are only few *in vivo* studies attempting to further explore this potential. For instance, it was shown that Z-VAD led to significant radiosensitization of breast and lung cancer xenografts.[43] Our *in vitro* experiments suggested that pan-caspase inhibitors might be useful to overcome chemoresistance in CRC, possibly by converting 5-FU-induced NF-κB signaling into a pro-death response. While Emricasan, the orally administrable sister compound of IDN-7314, was successful in clinical trials for the treatment of chronic liver diseases and liver transplantation,[44,45] here, we report for the first time that 5-FU and IDN-7314 can exert potent synergistic anti-tumor effects. In an *in vivo* murine CRC xenograft model, combination treatment led to reduced tumor masses and increased signs of tumor regression, which might be due to the induction of necroptosis in tumor cells. Examining tissue specimens from surgical CRC patients, we were able to identify a subgroup of tumors, which lacked signs of apoptotic death in response to 5-FU, but showed an improved response to combination treatment with Z-VAD. In line with our cell culture experiments, elevated levels of TNF-α and NF-κB were exclusively and components of the necrosome were preferably found in these necroptosis-sensitive cases. However, to which extent these markers might provide valuable information on the sensitivity to pro-necroptotic therapy needs to be investigated in a higher number of samples. In addition, standardized diagnostic testing, for example, using the tissue culture model, will be required to avoid unwanted side-effects due to caspase inhibition.

In summary, our results warrant the further evaluation of targeted necroptosis induction as a novel therapeutic strategy for CRC. Given that predictive diagnostic tests could identify apoptosis-resistant tumors, which might respond towards a pro-necroptotic treatment, caspase inhibitors might help to overcome chemoresistance in CRC.

MATERIALS AND METHODS

Materials

Human recombinant TNF-α was from ImmunoTools (Friesoythe, Germany). Propidium iodine and 5-FU were from Sigma Aldrich (Hamburg, Germany). Z-VAD-fmk, Z-DEVD-fmk, Z-VEID-fmk, Z-IETD-fmk and Necrostatin-1 were from Enzo Life Sciences (Loerrach, Germany). Necrosulfonamide and GSK'872 were from Calbiochem (Merck Millipore, Darmstadt, Germany). BV6 was generously provided by Genentech, Inc. (South San Francisco, CA, USA), IDN-7314 by Conatus Pharmaceuticals, Inc. (San Diego, CA, USA).

Cell culture

HCT116, HT29 and SW480 human CRC cell lines were obtained from ATCC (Manassas, VA, USA). ATCC provides standardized cell line authentication

© 2016 Macmillan Publishers Limited

utilizing short tandem repeat profiling. Within 4 weeks, all cell lines were expanded and frozen in aliquots. Cell lines were re-authenticated once before initial experiments and regularly tested for mycoplasma contamination as provided by the German Cancer Research Center (DKFZ) Core Facility (Heidelberg, Germany). Cells were maintained in RPMI-1640 medium (Biochrom, Berlin, Germany) containing 10% fetal calf serum (PAA Laboratories, GE Healthcare, Freiburg, Germany) and 1% penicillin/streptomycin at 5% CO_2 and 37 °C.

Cell viability assay

Cells were grown to subconfluence in 96-well plates (15 000–20 000 per well). After pre-treatment with Z-VAD (50 μM) and/or Necrostatin-1 (20 μM) for 2 h, BV6 (0.6 μM), TNF-α (25 ng/ml) or 5-FU (50 μg/ml) was added. After 48 h, remaining adherent cells were stained with crystal violet and absorption was measured using a microplate reader (Bio-Rad, Muenchen, Germany).

Transfection of short interference (si) RNA

For siRNA knockdown, HT29 cells were transfected with a pool of four individual siRNA sequences (siGENOME set of four upgrade, Dharmacon, GE Healthcare, Freiburg, Germany) at a final concentration of 50 nM. A non-specific siRNA served as a control (Dharmacon, GE Healthcare). After 24 h, cells were treated as indicated. Knockdown efficiencies were tested 48–72 h after transfection on protein and mRNA level (see Supplementary Figure 3).

Flow cytometry

In accordance with Vanden Berghe *et al.*,[46] apoptosis and necrosis were determined by flow cytometry (FACScalibur cytometer, BD Biosciences, Heidelberg, Germany). Briefly, non-permeabilized cells were washed and stained with propidium iodine, and cell permeability, size and granularity were analyzed. To measure the expression of cell-surface TNFR1, cells were incubated with fluorescently labeled anti-TNFR1 (SM1185F, Acris, Herford, Germany) or mouse IgG isotype control antibody for 1 h at room temperature. Data analysis was carried out using Cell Quest Software (BD Biosciences).

Electron microscopy

HT29 cells were grown on cover slips. After pre-treatment with Z-VAD (50 μM) for 2 h, cells were either stimulated with BV6 (0.6 μM) and TNF-α (25 ng/ml), or 5-FU (50 μg/ml) for the indicated durations. Cells were fixed in Karnovsky fixative for 2 h, postfixed with osmium tetroxide (1.5%) for 2 h, contrasted with uranyl acetate for 45 min, and embedded in araldite. Ultrathin sections (60–70 nM) were viewed in a Zeiss EM910 (Zeiss, Oberkochen, Germany). Photographs were taken with a slow-scan CCD camera (2 K, Zeiss).

Immunoblotting

Cell lysates were prepared and western blot analysis was conducted as previously described.[47] Protein extraction from paraffin tissue sections was performed using Qproteome FFPE Tissue Kit (QIAGEN, Hilden, Germany). The following antibodies were used: pH2AX (sc-101696, Santa Cruz, Heidelberg, Germany), PARP (556562, BD Biosciences), caspase 3 (IMG--144 A, Imgenex, Novus Biologicals, Abingdon, UK), cIAP1 (AF8181, R&D Systems, Wiesbaden, Germany), EDD (NB100-1591, Novus Biologicals), caspase 8 (551242, BD Pharmingen, Heidelberg, Germany), RIP1 (610458, BD Biosciences), RIP3 (NBP2-24588, Novus Biologicals), MLKL (NBP1-56729, Novus Biologicals), pMLKL (ab187091, Abcam, Cambridge, UK), FADD (610399, BD Biosciences), pIκBα (9246 S, Cell Signaling, Beverly, MA, USA), TNFR1 (sc-8436, Santa Cruz), p52 (3017, Cell Signaling), RelA (sc-105, Santa Cruz), and corresponding secondary antibodies (horseradish peroxidase-conjugated, Bio-Rad). Signal was developed using enhanced chemiluminescence detection system (GE Healthcare).

Co-immunoprecipitation

Cells were resuspended in lysis buffer containing 1% Triton and protease inhibitors for 15 min at 4 °C. After centrifugation, lysates were incubated with 30 μl beads (G-Sepharose-4B, Invitrogen, Thermo Fisher Scientific, Karlsruhe, Germany) and 5 μl of primary antibody against caspase 8 (sc-6136, Santa Cruz) or RIP1 (sc-7881, Santa Cruz) overnight at 4 °C. Beads were recovered by centrifugation and washed at least six times with lysis buffer before samples were analyzed by immunoblotting.

Nuclear extraction

Nuclear protein extraction was performed using 6×10^6 cells following the nuclear extract kit (Active Motif, La Hulpe, Belgium). Samples were analyzed by immunoblotting.

Quantitative real-time–polymerase chain reaction (qRT–PCR) analysis

qRT–PCR was performed as previously described.[48] The primer pairs used were: RIP1: 5′-AATTTCCCAGGCAGTTGTTG-3′ (forward), 5′-CATTTCCTGTT CCCTCTCCA-3′ (reverse), RIP3: 5′-AAGAGGAGCAGGTTCCACAA-3′ (forward), 5′-CCAGGACTTGGTGTTCCAGT-3′, TNFR1: 5′-ACCAAGTGCCACAAAGGAAC-3′ (forward), 5′-GTTTTCTGAAGCGGTGAAGG-3′ (reverse), Actin: 5′-CCTAAAAG CCACCCCACTTCTC-3′ (forward), 5′-ATGCTATCACCTCCCCTGTGTG-3′ (reverse), TNF-α: 5′-CCTGTGAGGAGGACGAACAT-3′ (forward), 5′-GGTTGAGGGTGT CTGAAGGA-3′ (reverse), IL-8: 5′-CAAGAGCCAGGAAGAAACCA-3′ (forward), 5′-ACTCCTTGGCAAAACTGCAC-3′ (reverse), CCL20: 5′-GCGCAAATCCAAAA CAGACT-3′ (forward), 5′-CAAGTCCAGTGAGGCACAAA-3′ (reverse), IκBα: 5′-GCTGATGTCAATGCTCAGGA-3′ (forward), 5′-CCCCACACTTCAACAGGAGT-3′ (reverse), XIAP: 5′-TGGGGTTCAGTTTCAAGGAC-3′ (forward), 5′-TGCAACC AGAACCTCAAGTG-3′ (reverse), $cFLIP_{long}$: 5′-CCTAGGAATCTGCCTGATAAT CGA-3′ (forward), 5′-TGGGATATACCATGCATACTGAGATG-3′ (reverse), cIAP1: 5′-GCATTTTCCCAACTGTCCAT-3′ (forward), 5′-ATTCGAGCTGCATGT GTCTG-3′ (reverse).

Enzyme-linked immunosorbent assay (ELISA) for detection of TNF-α

Supernatants from cultured cells were centrifuged for removal of dead cells. TNF-α was measured using Quantikine ELISA kit (R&D Systems).

Animal studies

Six-week-old male athymic CD1 nude mice (Charles River, Erkrath, Germany) were injected subcutaneously with 1×10^6 HT29 cells in 200 μl phosphate-buffered saline in the right and left flank using a 27-gauge needle. As soon as tumors were palpable, animals were block-randomized into four groups of treatment ($n = 8$) receiving the following substances: control group (dimethyl sulfoxide, DMSO), 5-FU (40 mg/kg per week), IDN-7314 (120 mg/kg per week) or 5-FU and IDN-7314 (40 and 120 mg/kg per week, respectively). Animals received a first intraperitoneal injection of either DMSO (50% in phosphate-buffered saline) or IDN-7314 (40 mg/kg in 50% DMSO, 150 μl), followed by a second injection of either DMSO (4% in phosphate-buffered saline) or 5-FU (13.3 mg/kg in 4% DMSO, 200 μl). Tumor volumes were measured using the ellipsoid formula (length × width × height × ½). After 3 weeks of treatment, animals were killed. Tumors were formalin-fixed and paraffin-embedded, and sections were used for histological and immunohistochemical analysis. Animal work was carried out in accordance with the NIH guidelines Guide for the Care and Use of Laboratory Animals, and the protocol was approved by the German animal welfare authorities (Regierungspraesidium Karlsruhe, permit number: 35-9185.81/G-103/11). All efforts were made to minimize suffering.

Histology and immunohistochemistry

Xenograft tumors were formalin-fixed for 24 h. After paraffin embedment, hematoxylin and eosin-stained slices were created for histopathological analysis. Sclerotic and necrotic areas within the tumor bed (loss of tumor cells, increase of inflammatory cells and fibroblasts) were interpreted as signs of regression. Regressive areas were quantified in relation to each tumor's size using the Aperio Image Scope software (Leica Biosystems, Wetzlar, Germany). Immunohistochemical staining of Ki-67/MIB1 (3,3′-diaminobenzidine) was performed and positive nuclei were quantified via computer-assisted analysis (see below).

Culture of tissue slices

Tissue samples were provided by the tissue bank of the National Center for Tumor Diseases (NCT, Heidelberg, Germany) and collected from 13 subjects receiving surgical therapy in the years 2012–14 (University Hospital Heidelberg, Heidelberg, Germany). Immediately after surgical

© 2016 Macmillan Publishers Limited

removal, the tissue was kept in Dulbecco's modified Eagle's medium (Biochrom, Berlin, Germany) on ice and processed as previously described.[48] Briefly, 300-μm thin slices were created using a vibrating blade microtome (Leica) and cultured on porous filter membranes in Dulbecco's modified Eagle's medium containing 1% penicillin/streptomycin at 5% CO_2 and 37 °C. After pre-treatment with Z-VAD (50 μm) for 2 h and 5-FU (500 μg/ml) for 48 h, supernatants were centrifuged and LDH levels were quantified by the Department of Laboratory Services, University Hospital Heidelberg. Tissue slices were formalin-fixed and paraffin-embedded, and the tumor content (mm^2) of hematoxylin and eosin-stained sections was analyzed using Aperio Image Scope (see below). Immunohistochemical staining of cleaved Caspase 3 (559565, BD Pharmingen) and RelA (sc-372, Santa Cruz) was performed and quantified by two independent pathologists. Usage of tumor tissue for research purpose was approved by the local ethics committee of the University Hospital of Heidelberg (permit number: 206/2005). All data were analyzed anonymously; written informed consent from donors or the next of kin was obtained for research use of these samples.

Software-assisted image analysis

Histological slides were scanned for digital analysis using an Aperio CS scanner. Areas of interest were manually annotated (tumor bed, regressive changes) by an experienced pathologist followed by measurement in default settings by the Aperio Image Scope software (v11.0.2.725, Leica Biosystems). Ki-67-proliferative rates were obtained using the Nuclear analysis tool (Aperio Image Scope). Here, tumor nuclei were identified by size and shape (hematoxylin), and positive and negative nuclei were quantified by the intensitiy of staining (DAB).

Statistical analysis

Statistical significance was assessed by two-sided Student's *t*-test. Sample size, number of technical or biological replicates, and statistical test results are specified in each figure legend.

CONFLICT OF INTEREST

The authors declare no conflict of interest.

ACKNOWLEDGEMENTS

We are grateful to Marina Gernold, Martina Keith, Katarina Duglova and Scott Oliver for excellent technical assistance. We thank Sylvia Kaden for technical assistance during electron microscopy. We thank the tissue bank of the Center for National Tumor Disease (NCT, Heidelberg, Germany) for providing CRC tissues, and Sarah Meßnard and David Jansen for technical assistance during immunohistochemistry. This study was supported by a grant from the Manfred-Stolte-Foundation to WR, and by the Rahel Goitein-Straus Program of the Medical Faculty of Heidelberg (fellowship to MOM).

REFERENCES

1 Ferlay J, Soerjomataram I, Dikshit R, Eser S, Mathers C, Rebelo M *et al.* Cancer incidence and mortality worldwide: Sources, methods and major patterns in GLOBOCAN 2012. *Int J Cancer* 2014; **136**: E359–E386.
2 Hagan S, Orr MC, Doyle B. Targeted therapies in colorectal cancer-an integrative view by PPPM. *EPMA J* 2013; **4**: 3.
3 Marshall JL, Haller DG, de Gramont A, Hochster HS, Lenz HJ, Ajani JA *et al.* Adjuvant therapy for stage II and III colon cancer: Consensus Report of the International Society of Gastrointestinal Oncology. *Gastrointest Cancer Res* 2007; **1**: 146–154.
4 Tournigand C, Andre T, Achille E, Lledo G, Flesh M, Mery-Mignard D *et al.* FOLFIRI followed by FOLFOX6 or the reverse sequence in advanced colorectal cancer: a randomized GERCOR study. *J Clin Oncol* 2004; **22**: 229–237.
5 Douillard JY, Sobrero A, Carnaghi C, Comella P, Diaz-Rubio E, Santoro A *et al.* Metastatic colorectal cancer: integrating irinotecan into combination and sequential chemotherapy. *Ann Oncol* 2003; **14**: ii7–12.
6 Wilson PM, Ladner RD, Lenz HJ. Predictive and prognostic markers in colorectal cancer. *Gastrointest Cancer Res* 2007; **1**: 237–246.
7 Hanahan D, Weinberg RA. Hallmarks of cancer: the next generation. *Cell* 2011; **144**: 646–674.
8 Cooks T, Pateras IS, Tarcic O, Solomon H, Schetter AJ, Wilder S *et al.* Mutant p53 prolongs NF-kappaB activation and promotes chronic inflammation and inflammation-associated colorectal cancer. *Cancer Cell* 2013; **23**: 634–646.
9 Kroemer G, Galluzzi L, Vandenabeele P, Abrams J, Alnemri ES, Baehrecke EH *et al.* Classification of cell death: recommendations of the Nomenclature Committee on Cell Death 2009. *Cell Death Differ 2009* **16**: 3–11.
10 Kreuzaler P, Watson CJ. Killing a cancer: what are the alternatives? *Nat Rev Cancer* 2012; **12**: 411–424.
11 Zhou W, Yuan J. Necroptosis in health and diseases. *Semin Cell Dev Biol* 2014; **35**: 14–23.
12 Christofferson DE, Li Y, Yuan J. Control of life-or-death decisions by RIP1 kinase. *Annu Rev Physiol* 2014; **76**: 129–150.
13 Degterev A, Hitomi J, Germscheid M, Ch'en IL, Korkina O, Teng X *et al.* Identification of RIP1 kinase as a specific cellular target of necrostatins. *Nat Chem Biol* 2008; **4**: 313–321.
14 Micheau O, Tschopp J. Induction of TNF receptor I-mediated apoptosis via two sequential signaling complexes. *Cell* 2003; **114**: 181–190.
15 Darding M, Meier P. IAPs: guardians of RIPK1. *Cell Death Differ* 2012; **19**: 58–66.
16 Vandenabeele P, Galluzzi L, Vanden Berghe T, Kroemer G. Molecular mechanisms of necroptosis: an ordered cellular explosion. *Nat Rev Mol Cell Biol* 2010; **11**: 700–714.
17 Hitomi J, Christofferson DE, Ng A, Yao J, Degterev A, Xavier RJ *et al.* Identification of a molecular signaling network that regulates a cellular necrotic cell death pathway. *Cell* 2008; **135**: 1311–1323.
18 He S, Wang L, Miao L, Wang T, Du F, Zhao L *et al.* Receptor interacting protein kinase-3 determines cellular necrotic response to TNF-alpha. *Cell* 2009; **137**: 1100–1111.
19 Laukens B, Jennewein C, Schenk B, Vanlangenakker N, Schier A, Cristofanon S *et al.* Smac mimetic bypasses apoptosis resistance in FADD- or caspase-8-deficient cells by priming for tumor necrosis factor alpha-induced necroptosis. *Neoplasia* 2011; **13**: 971–979.
20 Sun L, Wang H, Wang Z, He S, Chen S, Liao D *et al.* Mixed lineage kinase domain-like protein mediates necrosis signaling downstream of RIP3 kinase. *Cell* 2012; **148**: 213–227.
21 Kaiser WJ, Sridharan H, Huang C, Mandal P, Upton JW, Gough PJ *et al.* Toll-like receptor 3-mediated necrosis via TRIF, RIP3, and MLKL. *J Biol Chem* 2013; **288**: 31268–31279.
22 Tenev T, Bianchi K, Darding M, Broemer M, Langlais C, Wallberg F *et al.* The Ripoptosome, a signaling platform that assembles in response to genotoxic stress and loss of IAPs. *Mol Cell* 2011; **43**: 432–448.
23 Feoktistova M, Geserick P, Kellert B, Dimitrova DP, Langlais C, Hupe M *et al.* cIAPs block ripoptosome formation, a RIP1/caspase-8 containing intracellular cell death complex differentially regulated by cFLIP isoforms. *Mol Cell* 2011; **43**: 449–463.
24 Biton S, Ashkenazi A. NEMO and RIP1 control cell fate in response to extensive DNA damage via TNF-alpha feedforward signaling. *Cell* 2011; **145**: 92–103.
25 Christofferson DE, Li Y, Hitomi J, Zhou W, Upperman C, Zhu H *et al.* A novel role for RIP1 kinase in mediating TNFalpha production. *Cell Death Dis* 2012; **3**: e320.
26 Jouan-Lanhouet S, Riquet F, Duprez L, Vanden Berghe T, Takahashi N, Vandenabeele P. Necroptosis, in vivo detection in experimental disease models. *Semin Cell Dev Biol* 2014; **35**: 2–13.
27 Wang W, Cassidy J, O'Brien V, Ryan KM, Collie-Duguid E. Mechanistic and predictive profiling of 5-Fluorouracil resistance in human cancer cells. *Cancer Res* 2004; **64**: 8167–8176.
28 Fulda S. Therapeutic exploitation of necroptosis for cancer therapy. *Semin Cell Dev Biol* 2014; **35**: 51–56.
29 Han W, Li L, Qiu S, Lu Q, Pan Q, Gu Y *et al.* Shikonin circumvents cancer drug resistance by induction of a necroptotic death. *Mol Cancer Ther* 2007; **6**: 1641–1649.
30 Grassilli E, Narloch R, Federzoni E, Ianzano L, Pisano F, Giovannoni R *et al.* Inhibition of GSK3B bypass drug resistance of p53-null colon carcinomas by enabling necroptosis in response to chemotherapy. *Clin Cancer Res* 2013; **19**: 3820–3831.
31 Steinhart L, Belz K, Fulda S. Smac mimetic and demethylating agents synergistically trigger cell death in acute myeloid leukemia cells and overcome apoptosis resistance by inducing necroptosis. *Cell Death Dis* 2013; **4**: e802.
32 Dunai ZA, Imre G, Barna G, Korcsmaros T, Petak I, Bauer PI *et al.* Staurosporine induces necroptotic cell death under caspase-compromised conditions in U937 cells. *PLoS ONE* 2012; **7**: e41945.
33 Lin Y, Devin A, Rodriguez Y, Liu ZG. Cleavage of the death domain kinase RIP by caspase prompts TNF-induced apoptosis. *Genes Dev* 1999; **13**: 2514–2526.
34 Varfolomeev E, Blankenship JW, Wayson SM, Fedorova AV, Kayagaki N, Garg P *et al.* IAP antagonists induce autoubiquitination of c-IAPs, NF-kappaB activation, and TNFalpha-dependent apoptosis. *Cell* 2007; **131**: 669–681.

© 2016 Macmillan Publishers Limited

35 Festjens N, Berghe TV, Cornelis S, Vandenabeele P. RIP1, a kinase on the crossroads of a cell's decision to live or die. *Cell Death Differ* 2007; **14**: 400–410.
36 Lamkanfi M, Declercq W, Vanden Berghe T, Vandenabeele P. Caspases leave the beaten track: caspase-mediated activation of NF-kappaB. *J Cell Biol* 2006; **173**: 165–171.
37 Chaudhary PM, Eby MT, Jasmin A, Kumar A, Liu L, Hood L. Activation of the NF-kappaB pathway by caspase 8 and its homologs. *Oncogene* 2000; **19**: 4451–4460.
38 Shikama Y, Yamada M, Miyashita T. Caspase-8 and caspase-10 activate NF-kappaB through RIP, NIK and IKKalpha kinases. *Eur J Immunol* 2003; **33**: 1998–2006.
39 Staal J, Bekaert T, Beyaert R. Regulation of NF-kappaB signaling by caspases and MALT1 paracaspase. *Cell Res* 2011; **21**: 40–54.
40 McComb S, Shutinoski B, Thurston S, Cessford E, Kumar K, Sad S. Cathepsins limit macrophage necroptosis through cleavage of Rip1 kinase. *J Immunol* 2014; **192**: 5671–5678.
41 Zhang L, Blackwell K, Workman LM, Chen S, Pope MR, Janz S *et al.* RIP1 cleavage in the kinase domain regulates TRAIL-induced NF-kappaB activation and lymphoma survival. *Mol Cell Biol* 2015; **35**: 3324–3338.
42 Probst BL, Liu L, Ramesh V, Li L, Sun H, Minna JD *et al.* Smac mimetics increase cancer cell response to chemotherapeutics in a TNF-alpha-dependent manner. *Cell Death Differ* 2010; **17**: 1645–1654.
43 Moretti L, Kim KW, Jung DK, Willey CD, Lu B. Radiosensitization of solid tumors by Z-VAD, a pan-caspase inhibitor. *Mol Cancer Ther* 2009; **8**: 1270–1279.
44 Linton SD, Aja T, Armstrong RA, Bai X, Chen LS, Chen N *et al.* First-in-class pan caspase inhibitor developed for the treatment of liver disease. *J Med Chem* 2005; **48**: 6779–6782.
45 Shiffman ML, Pockros P, McHutchison JG, Schiff ER, Morris M, Burgess G. Clinical trial: the efficacy and safety of oral PF-03491390, a pancaspase inhibitor - a randomized placebo-controlled study in patients with chronic hepatitis C. *Aliment Pharmacol Ther* 2010; **31**: 969–978.
46 Vanden Berghe T, Grootjans S, Goossens V, Dondelinger Y, Krysko DV, Takahashi N *et al.* Determination of apoptotic and necrotic cell death in vitro and in vivo. *Methods* 2013; **61**: 117–129.
47 Fuchs D, Metzig M, Bickeboller M, Brandel C, Roth W. The Gbeta5 protein regulates sensitivity to TRAIL-induced cell death in colon carcinoma. *Oncogene* 2014; **34**: 2753–2763.
48 Fassl A, Tagscherer KE, Richter J, Berriel Diaz M, Alcantara Llaguno SR, Campos B *et al.* Notch1 signaling promotes survival of glioblastoma cells via EGFR-mediated induction of anti-apoptotic Mcl-1. *Oncogene* 2012; **31**: 4698–4708.

Supplementary Information accompanies this paper on the Oncogene website (http://www.nature.com/onc)

© 2016 Macmillan Publishers Limited